Energy Gap in Nuclear Matter. I. Extended Theory*

E. M. HENLEY AND L. WILETS
University of Washington, Seattle, Washington
(Received 10 October 1963)

The Bogoliubov condition of compensation of dangerous diagrams is invoked to derive a generalized energy-gap equation of the BCS form, but with a renormalized pairing interaction and renormalized single-particle energies. The second-order contributions to the renormalized pairing interaction are found to be significant, contrary to popular belief. It is stressed that the self-consistent solution of the energy-gap equation yields qualitatively and quantitatively different results than a perturbative evaluation of the energy spectrum following a Bogoliubov-Valatin transformation characterized by the lowest order BCS gap parameters. The dependence of the energy gap on high-order corrections is studied in one and three dimensions for simple potentials; for some values of the potential parameters, no solution to the gap equation exists. Finally, the energy gap is studied in nuclear matter. We include the scattering in both singlet and triplet states of particle-hole pairs which can be neutron-neutron, neutron-proton, or proton-proton. The interaction is taken to be a sum of separable potentials which reproduce the s-wave phase shift. Because of the short-range repulsion that is included, we sum an infinite set of particle-particle diagrams which replaces the second-order potential vertices by T matrices. The higher order effects studied increase the energy gap by a large factor, especially when the lowest order BCS gap is calculated to be small. Nevertheless, the qualitative conclusion remains that the energy gap in infinite nuclear matter appears to be considerably smaller than that in the heaviest nuclei.

I. INTRODUCTION

In recent years, impressive progress has been made in understanding nuclear spectra in terms of phenomenological, two-body potentials. This work has been spurred by the Copenhagen group[1] which specifically employs a short-range pairing (seniority[2]) force and a longer range quadrupole force. The forces are characterized by relatively few parameters, each of which may vary smoothly with A.

The pairing interaction—which concerns us here—gives rise to an energy gap in the spectra of even-even nuclei consistent with observation. Other manifestations of the pairing force include even-odd ground-state mass differences and the reduction of nuclear rotational moments of inertia from the rigid value. In Fig. 1 are displayed the pairing energies deduced from empirical even-odd mass differences.[3] These numbers are approximately half the energy gap in even-even nuclei. The regions away from closed shells (that is, where the nuclei have intrinsic deformations and shell-structure degeneracies are effectively broken) exhibit considerable regularity in the pairing energy. Except near closed shells, the pairing energy is seen to decrease slowly with increasing A.

Much less progress has been made in understanding the origin of the phenomenological, relatively strong, short-range pairing force in terms of two-body forces derived from scattering experiments. In particular, Emery and Sessler[4] solved the Bardeen-Cooper-Schrieffer[5] integral equation for an infinite system employing the Gammel-Thaler[6] potential. This potential not only fits two-body scattering data up to a few hundred MeV, but also has been successful in reproducing the bulk properties of nuclear matter. Although the BCS equation is capable of yielding a finite gap for an infinite system, Emery and Sessler found the gap in nuclear matter to be three orders of magnitude smaller than the gap observed in the heaviest nuclei. Qualitatively similar results have been obtained by Brueckner *et al.*,[7] who (incorrectly) used the nuclear matter two-body K matrix instead of the bare two-body potential in the BCS equation. In a companion paper,[8] more recent calculations based on a variety of internucleonic potentials satisfying s-wave scattering data are shown to yield qualitatively similar results. The conclusion that the BCS theory predicts a very small gap for infinite nuclear matter appears not to be sensitively dependent upon the special choice of potentials.

We can understand physically why the BCS integral equation yields a negligibly small value for the energy gap. The dominant potential-matrix elements are between pairs of particles at the Fermi surface (and, of course, with zero center-of-mass momentum). These correspond crudely to the scattering of 80-MeV particles in the center-of-mass system or 160-MeV incident energy in a laboratory experiment. At these high energies (the highest available to nucleon pairs in a Fermi-gas model of the nucleus) the repulsive core is effective in virtually destroying the attraction. The repulsive core, however, is necessary for understanding nuclear saturation.

* Supported in part by the U. S. Atomic Energy Commission under Contract A.T.(45-1)-1388, program B.

[1] See, for example, L. S. Kisslinger and R. A. Sorensen, Kgl. Danske Videnskab. Selskab, Mat. Fys. Medd. **32**, No. 9 (1960).

[2] G. Racah, Phys. Rev. **63**, 367 (1943).

[3] P. E. Nemirovsky and Yu. V. Adamchuk, Nucl. Phys. **39**, 551 (1962).

[4] V. J. Emery and A. M. Sessler, Phys. Rev. **119**, 248 (1960).

[5] J. Bardeen, L. N. Cooper, and J. R. Schrieffer, Phys. Rev. **108**, 1175 (1957). This paper will be referred to as BCS hereafter.

[6] J. L. Gammel and R. M. Thaler, Phys. Rev. **107**, 291 (1957).

[7] K. A. Brueckner, T. Soda, P. W. Anderson, and P. Morel, Phys. Rev. **118**, 1442 (1960).

[8] R. Kennedy, L. Wilets, and E. M. Henley, following paper, Phys. Rev. **133**, B1131 (1964). This will henceforth be referred to as paper II.

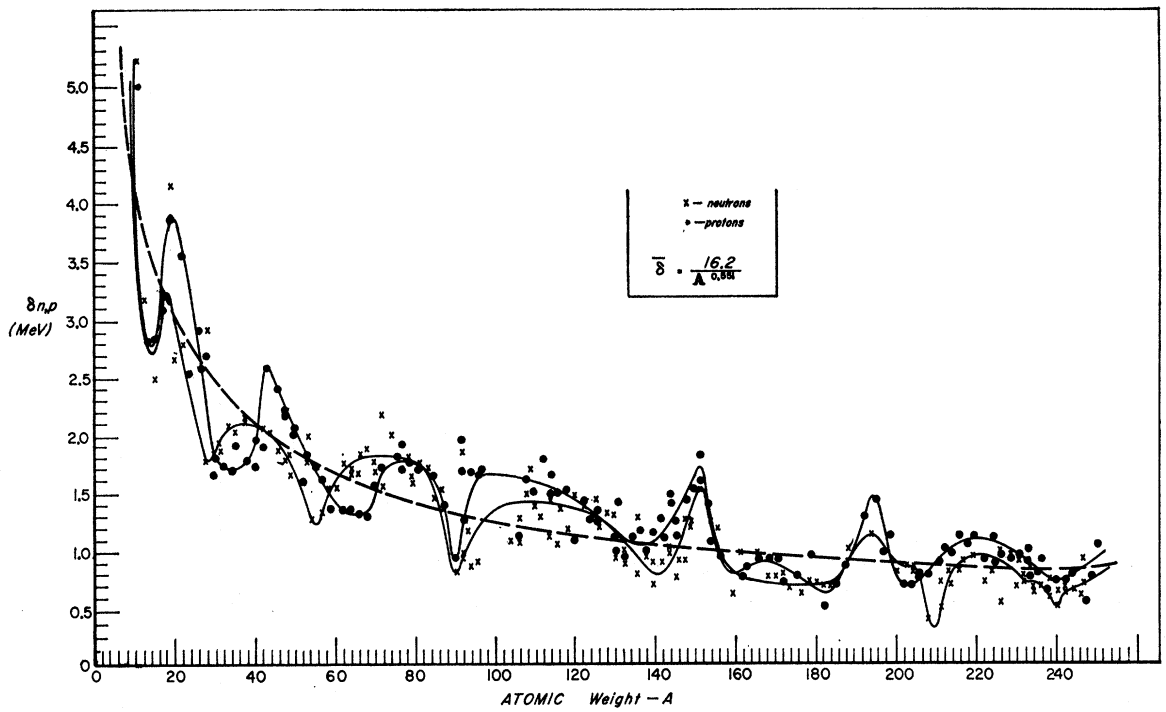

FIG. 1. Pairing energy of two nucleons deduced from even-odd mass differences, reproduced from Nemirovsky and Adamchuk (Ref. 3). The black circles (δ_p) refer to protons, the open circles (δ_n) to neutrons. $\bar{\delta}$ is an average empirical fit. The pairing energy δ is approximately, but not identically, equal to the energy gap parameter Δ.

We conclude that there are three nonexclusive alternatives in understanding the magnitude of the gap in heavy nuclei:

(1) The gap is a finite size (e.g., surface) effect which either vanishes or becomes negligibly small in infinite nuclear matter. This is the interpretation, for example, of Nemirovsky and Adamchuk[3] in fitting the pairing energy to an $A^{-0.551}$ law.

(2) The energy gap in nuclear matter is comparable with the gap in heavy nuclei, but further corrections must be applied to the BCS theory in order to calculate the gap accurately.

(3) The BCS theory is not relevant to the nuclear energy-gap problem.

Alternative (1) is currently being investigated, and results will be reported in a subsequent paper. We will ignore the third alternative for the present. The present work is addressed to an examination of (2), namely, the investigation of higher order corrections to the BCS theory.

In Sec. II, the Bogoliubov-Valatin canonical transformation is introduced. The parameters of the transformation are determined by the "principle of compensation of dangerous diagrams." This condition leads to a generalized BCS integral equation which contains a renormalized pairing interaction and renormalized single-particle energies. In a previous communication[9] we demonstrated that the second-order (in the transformed Hamiltonian) corrections to the pairing interaction are not exponentially small—as claimed by Bogoliubov, Tolmachev, and Shirkov[10]—and for simple attractive interactions can be important not only in determining the magnitude of the gap, but even its existence. The dominant second-order effects correspond, in perturbation language, to the intermediate scattering of a particle-hole pair.

In Sec. III, we consider the effect on the generalized BCS equation of including infinite sums of particle-hole and particle-particle diagrams in a one-dimensional model with a simple, separable interaction. The inclusion of second-order interaction terms for simple three-dimensional potentials, reported previously,[9] is summarized in Sec. IV.

The topic of primary interest is presented in Sec. V. This is the evaluation of the energy gap in nuclear matter. It is carried out for a sum of separable potentials, consisting of a short-range repulsive shell and a longer range attraction, adjusted to fit two-body scattering data. We have not restricted ourselves to scattering in singlet states only, but have included triplet forces as well. The calculation for the energy gap is carried out with the generalized BCS equation; it includes effects of particle-particle interactions to all orders and particle-hole forces to second order. The

[9] E. M. Henley and L. Wilets, Phys. Rev. Letters **11**, 326 (1963).

[10] N. N. Bogoliubov, V. V. Tolmachev, and D. V. Shirkov, *A New Method in the Theory of Superconductivity* (Consultants Bureau, Inc., New York, 1959), Chap. VII.

results indicate that the second-order corrections are very important to the magnitude of the calculated gap, but whether or not the gap is appreciable in size depends crucially on the assumed value of the effective mass.

A critique of the calculations as well as suggested further areas of investigation is included in the conclusion.

II. COMPENSATION OF DANGEROUS DIAGRAMS

A. General Considerations

The perturbation expansion of the ground-state energy of the many-body system involves the evaluation of integrals (diagrams) containing energy denominators which may vanish. The vanishing of a denominator is not catastrophic unless the resulting singularity is nonintegrable. The most serious (in the sense of phase space) vanishing denominators yet discovered occur when propagator lines have pair-wise equal and opposite momenta, and all lie at the Fermi surface. Even in this case, the singularities are integrable in each order of perturbation theory, but infinite sums of such diagrams —such as are normally summed by a T matrix—do lead to (logarithmically) divergent results.

Bogoliubov[11] has termed as "dangerous" that class of energy denominators which can lead to divergences. In order to circumvent divergence problems, he has proposed a canonical transformation which introduces quasiparticle operators in place of particle operators. The most divergent propagators in the perturbation expansion of the transformed representation consists of an isolated pair of quasiparticle lines. The principle of "compensation of dangerous diagrams," expounded by Bogoliubov,[11] is that the *sum* of all diagrams leading to an isolated pair must vanish for each value of the pair-momentum. When this condition can be satisfied nontrivially, the quasiparticle energies which appear in the propagators are always greater than some minimum value $\Delta>0$. Then one *anticipates* that perturbation theory can be applied without danger of divergences reappearing. Although no singularities of any kind occur in any order, one must still be prepared for the possible appearance of singularities in infinite sums of the type included in T matrices.

B. The Hamiltonian

We consider a system of nuclear matter consisting of uncharged nucleons (neutrons and neutral "protons") described by the Hamiltonian

$$H=\sum_{1}\epsilon_{k_1}a_1^{\dagger}a_1 + \tfrac{1}{4}\sum_{1,1',2,2'}\delta_{1'+2',1+2}\langle 1'2'|V|1\,2\rangle a_{1'}^{\dagger}a_{2'}^{\dagger}a_2a_1, \quad (2.1a)$$

where the numeral (n) stands for the set $(\mathbf{k}_n,s_n,t_n)$, with $\mathbf{k}_n$ the vector momentum, s_n the z component of spin, and t_n the third component of isospin. Here $\epsilon_k=(\hbar^2k^2/2m)-\mu$ is the kinetic energy of a particle measured relative to the chemical potential μ, which in lowest order is given by $\hbar^2k_F^2/2m$. The chemical potential (=Fermi energy) is introduced as a Lagrangian multiplier to assure the conservation of the mean number of particles when the approximations do not guarantee this conservation. The potential is taken to be real and to satisfy charge invariance, but may be spin-dependent. The interaction $\langle 1'2'|V|1\,2\rangle$ is the direct minus the exchange integral, such that

$$\langle 1'2'|V|1\,2\rangle=-\langle 1'2'|V|2\,1\rangle. \quad (2.1b)$$

The a's satisfy the Fermion anticommutation relations

$$[a_n,a_n']_+=[a_n^{\dagger},a_{n'}^{\dagger}]_+=0,$$
$$[a_n^{\dagger},a_{n'}]_+=\delta_{n,n'}. \quad (2.2)$$

C. The Bogoliubov-Valatin Transformation

We introduce a slight generalization of the Bogoliubov-Valatin[11] transformation, which consists in replacing the Fermion annihilation and creation operators a_{ks} and $a_{ks}^{\dagger}$ by the quasiparticle operators α_{ks} and $\alpha_{ks}^{\dagger}$ defined by

$$a_{ks}=u_{ks}\alpha_{ks}+v_{-k-s}\alpha_{-k-s}^{\dagger},$$
$$a_{ks}^{\dagger}=u_{ks}\alpha_{ks}^{\dagger}+v_{-k-s}\alpha_{-k-s}. \quad (2.3)$$

It can be shown that u and v may be chosen real and that the transformation is canonical if

$$u_{ks}=u_{-k-s},$$
$$v_{ks}=-v_{-k-s}, \quad (2.4)$$
$$u_{ks}^2+v_{ks}^2=1.$$

Then the operators α_n and $\alpha_n^{\dagger}$ obey the same anticommutation rules as the operators a_n and $a_n^{\dagger}$.

Because we are dealing with equal densities of neutrons and protons, we have assumed u and v to be independent of isospin. In actual heavy nuclei, the neutron and proton densities are quite different and so are the corresponding neutron and proton Fermi energies. If the two Fermi energies in actual nuclei were equal, one could consider a transformation which mixes proton and neutron operators. This would correspond to pairing neutrons to protons (with equal magnitude and oppositely directed momenta) rather than neutrons to neutrons and protons to protons. The phase space available to a neutron-proton pair coupled to zero total spin and momentum is twice as great as for like nucleons. The phase space enters crucially in the energy-gap condition. However, when the neutron and proton Fermi momenta are different, neutron-proton pairs no longer are dangerous, since their energies cannot vanish simultaneously. Although we will not consider explicit neutron-proton pairing, we will want to include other

[11] N. N. Bogoliubov, Zh. Eksperim. i Teor. Fiz. **34**, 58 (1958) [English transl.: Soviet Phys.—JETP **34**, 41 (1958)]; J. G. Valatin, Nuovo Cimento **7**, 794 (1958).

effects arising from the interactions between neutrons and protons; for these purposes the equal density approximation will be maintained.

The unperturbed ground, or vacuum, state $|0\rangle$ of the quasiparticle system is defined by

$$\alpha_n|0\rangle=0. \tag{2.5}$$

The transformation (2.3) is called "normal" or "trivial" if

$$\begin{aligned} u_{\mathbf{k}s}&=0, \\ |v_{\mathbf{k}s}|&=1, \end{aligned} \quad \epsilon_{\mathbf{k}}<0; \qquad \begin{aligned} u_{\mathbf{k}s}&=1, \\ v_{\mathbf{k}s}&=0, \end{aligned} \quad \epsilon_{\mathbf{k}}>0. \tag{2.6}$$

In this case, the vacuum state of the quasiparticles is just the Fermi sea, with $\alpha_{\mathbf{k}st}^\dagger$ representing a particle creation (hole annihilation) operator for $\mathbf{k}$ above the Fermi sea or a hole creation (particle annihilation) operator for $\mathbf{k}$ below the Fermi sea.

1. Potential Vertices

Direct substitution of the transformation (2.3) into the Hamiltonian (2.1) gives the transformed Hamiltonian. The ground-state energy of the transformed system can be computed by summing the contributions of all vacuum-to-vacuum connected diagrams generated by the transformed Hamiltonian. These diagrams can be constructed with the aid of the following rules:

In Fig. 2(a) we have drawn what we shall refer to as the "standard" potential vertex. The operators reading from right to left in Eq. (2.1) are associated with the legs read counterclockwise beginning at the lower right. The standard vertex contributes a factor

$$(\tfrac{1}{4}\delta_{1'+2',1+2}\langle 1'2'|\,V\,|1\,2\rangle)(u_{1'}u_{2'}u_2u_1).$$

Other *distinct* vertices can be generated from the standard one by rotating the legs about the vertex point from one side of the vertical to the other. A new diagram so obtained contains the same potential matrix element as the standard vertex. The remaining factors, or weight factors as we will call them, are given as follows:

(1) In rotating a leg, do not cross the lower dotted line.

(2) The arrows remain fixed on a leg; that is, the right-left sense of an arrow reverses in crossing the upper vertical. This assures two arrows into, and two arrows out of, each vertex.

(3) Crossing the upper vertical changes the leg indices from $\mathbf{k}$, s, t to $-\mathbf{k}$, $-s$, t; the t index remains unchanged. This assures conservation of linear momentum and z component of spin across a vertex. Quasiparticle number is not conserved. If, as a mnemonic, we think of an arrow to the left as meaning a quasiparticle and an arrow to the right as an antiquasiparticle, then quasiparticle number can be thought of as conserved independently for neutrons and protons at a vertex. If (n) denotes $(\mathbf{k}_n,s_n,t_n)$, we will mean by $(-n)$ the set $(-\mathbf{k}_n,-s_n,+t_n)$.

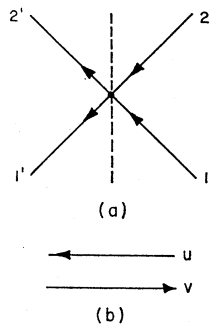

FIG. 2. Standard diagrams. (a) is the standard potential vertex; (b) illustrates how the partial weight factors u and v are associated with arrows pointing to the left and right, respectively.

(4) If one rotated leg crosses another, the vertex weight factor is multiplied by (-1).

(5) The vertex weight factor contains the product of four u's and v's, one for each leg according to whether the arrow points to the left or to the right, respectively [see Fig. 2(b)].

Two legs connected to the same vertex may be joined (contracted) into a loop according to the following rules.

(6) One leg must come from the right, and one from the left, of the (not necessarily standard) diagram. Both legs must bear identical indices.

(7) The relative position of the legs must be obtainable from the standard diagram without having switched (crossed) the pair.

(8) The weight factor associated with the pair is now determined by interchanging the legs of the loop (with *no* accompanying sign change) and then applying rule (5).

2. Kinetic-Energy Vertices

The transformed kinetic-energy operator assumes the form

$$\sum_{\mathbf{k}st}\epsilon_k[(u_{\mathbf{k}s}^2-v_{\mathbf{k}s}^2)\alpha_{\mathbf{k}st}^\dagger\alpha_{\mathbf{k}st} +u_{\mathbf{k}s}v_{-\mathbf{k}-s}(\alpha_{\mathbf{k}st}^\dagger\alpha_{-\mathbf{k}-st}^\dagger+\alpha_{-\mathbf{k}-st}\alpha_{\mathbf{k}st})+v_{\mathbf{k}s}^2]. \tag{2.7}$$

The terms involving uv factors play the same role in the perturbation expansion of the ground state as does the potential. Diagrammatically they give rise to wedge vertices, opening to the right or left. Each such vertex has associated with it the factor ϵ_k multiplied by a weight factor obtained by applying rules (1)–(5) above to the standard diagram given in Fig. 3. Only the wedge-type kinetic vertices are to be considered on a par with the potential vertices.

3. Propagators

Legs from different vertices labeled with the same index $(\mathbf{k},s,t)$ may be connected by lines irrespective of

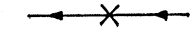

FIG. 3. Standard diagram for kinetic energy vertex.

FIG. 4. Diagrammatic representation of the generalized compensation condition.

the arrow direction. Every such line will have two arrows, each belonging to its respective vertex. If a pair of connecting lines cross, a factor (-1) must be included; this is consistent with rule (4). Between each pair of successive vertices (reading from right to left) there is associated a factor $(E_0-\sum \xi_k)^{-1}$, where the sum is taken over all propagator lines which exist simultaneously between the two vertices; E_0 is zero for the vacuum state, ξ_k is the coefficient of $\alpha_{ks\,t}^\dagger\alpha_{ks\,t}$,

$$\xi_k=(u_k^2-v_k^2)\epsilon_k. \tag{2.8}$$

(The spin index has been suppressed.) For the normal transformation, Eq. (2.6), this becomes $\xi_k=|\epsilon_k|$; in general, ξ_k is non-negative.

4. *The Compensation Condition*

It is sufficient, in order to compensate dangerous diagrams, to assert as a condition on the transformation, that the sum of all diagrams (Fig. 4) going from the vacuum to an isolated propagator pair $(\mathbf{k}, s, t, -\mathbf{k}-s, t)$ must vanish for each $(\mathbf{k},s,t)$. Diagrams which contain an intermediate state consisting of only an isolated pair need not be considered.

D. Lowest Order Diagrams: The BCS Integral Equation

Listed in Fig. 5 are all vacuum-to-pair diagrams through first order in the transformed interaction (potential and kinetic). Setting the sum of these diagrams

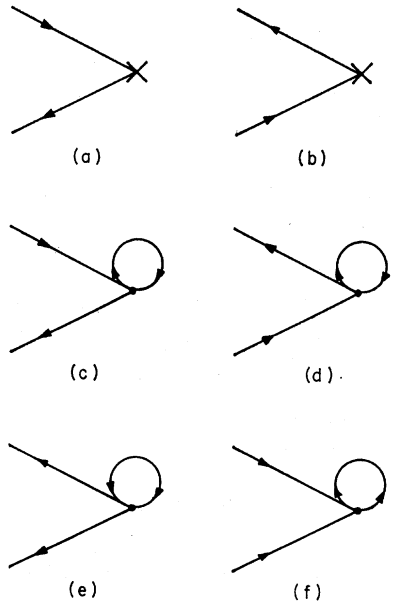

FIG. 5. Vacuum-to-pair diagrams through first order in the transformed interaction.

equal to zero, one finds

$$-2u_1v_1[\epsilon_1+\sum_{1'} v_{1'}^2\langle 1\,1'|V|1\,1'\rangle]$$
$$-(u_1^2-v_1^2)\tfrac{1}{2}\sum_{1'} u_{1'}v_{1'}\langle 1-1|V|1'-1'\rangle=0, \tag{2.9}$$

where the first term in the square brackets is $(a+b)$, the second $(c+d)$ and the next term of the equation is due to (e) and (f). Symmetries of the potential matrix elements have been used in combining terms. The sum over $(1')$ for (e) and (f) assumes the δ-function condition that $t_{1'}=t_1$.

The effect of diagrams (c) and (d) is to "dress" the single-particle energies by the usual Hartree-Fock potential energy. The dressed particle energies will be denoted by

$$\hat{\epsilon}_1=\epsilon_1+\sum_{1'} v_{1'}^2\langle 1\,1'|V|1\,1'\rangle. \tag{2.10}$$

In order that the density be the same as for a non-interacting gas, the chemical potential μ must be dressed as well.

Equation (2.9) can be cast into the standard BCS form by setting

$$\begin{pmatrix}u_k^2\\ v_k^2\end{pmatrix}=\frac{1}{2}\left(1\pm\frac{\hat{\epsilon}_k}{(\Delta_k^2+\hat{\epsilon}_k^2)^{1/2}}\right), \tag{2.11}$$

where we have assumed that $\hat{\epsilon}_k$ and Δ_k are independent of spin direction. This leads at once to the integral equation

$$\Delta_k=-\tfrac{1}{2}\sum_{k'}\frac{\Delta_{k'}}{(\Delta_{k'}^2+\hat{\epsilon}_{k'}^2)^{1/2}}G_{kk'}{}^0, \tag{2.12a}$$

where, to this order,

$$G_{kk'}{}^0\equiv\tfrac{1}{2}[\langle \mathbf{k}s, -\mathbf{k}-s|V|\mathbf{k}'s, -\mathbf{k}'-s\rangle$$
$$-\langle \mathbf{k}s, -\mathbf{k}-s|V|\mathbf{k}'-s, -\mathbf{k}'s\rangle]. \tag{2.12b}$$

The isospin index, which is constant throughout, has been suppressed. Note that G^0 is derivable from the singlet-spin part of the interaction only.

With some manipulation, the expectation value of a quasiparticle excited "state" $\alpha_{ks\,t}^\dagger|0\rangle$ can be shown to be given by

$$\hat{\xi}_k\equiv\langle 0|\alpha_{ks\,t}H\alpha_{ks\,t}^\dagger|0\rangle-\langle 0|H|0\rangle$$
$$=(\Delta_k^2+\hat{\epsilon}_k^2)^{1/2}. \tag{2.13}$$

$\hat{\xi}_k$ is to be interpreted—approximately—as an independent-quasiparticle excitational energy. We see that $\hat{\xi}_k\geq\Delta\equiv\Delta_{kF}$.

E. Generalized Energy-Gap Equation

With complete generality, we can group vacuum-to-pair diagrams (Fig. 4) into two classes, as shown in Fig. 6. Each arrow shown belongs to the vertex to which

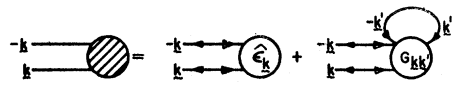

FIG. 6. Diagrammatic representation of the generalized integral equation. The vacuum-to-pair diagrams are grouped according to whether the external arrows point in the opposite or same directions. In the latter case, $G_{\mathbf{k}\mathbf{k}'}$, there is always at least one internal line with arrows pointing in opposite directions; this is explicitly indicated by the loop labeled $\mathbf{k}'$.

the line is attached inside the blob. Both solid and dashed arrow diagrams must be included in the sums. It is trivial to show that any diagram with both free leg arrows pointing out (or in) must have at least one internal line in which the two arrows point in opposite directions. (They need not loop in the direction shown, however.) The loop involves a factor $u_{\mathbf{k}'}v_{\mathbf{k}'}$; the sum over momenta $\mathbf{k}'$ is explicitly displayed by this separation. With these diagramatic definitions of $\hat{\epsilon}_{\mathbf{k}}$ and $G_{\mathbf{k}\mathbf{k}'}$, and retaining Eq. (2.11), the BCS integral equation now can be generalized formally to[9]

$$\Delta_{\mathbf{k}}=\tfrac{1}{2}\sum_{\mathbf{k}'}\frac{\Delta_{\mathbf{k}'}}{(\Delta_{\mathbf{k}'}^2+\hat{\epsilon}_{\mathbf{k}'}^2)^{1/2}}G_{\mathbf{k}\mathbf{k}'}. \tag{2.14}$$

The solution of this integral equation satisfies the compensation conditions to all orders in the transformed interaction. Our task now is to investigate higher order corrections to $\hat{\epsilon}$ and G.

There is a special property of the kinetic-energy vertices which we shall use in evaluating G to second order in the transformed interaction. In Fig. 7(a) is shown the only second-order diagram containing a kinetic-energy vertex. If, however, the second-order diagram 7(b) is added to 7(a), the sum can be shown to be of third order. This can be generalized to state that an nth-order diagram containing a kinetic-energy vertex [e.g., 7(d)] plus the same order "potential-loop" diagram [e.g., 7(e)] are of $(n+1)$st order. Consider the sequence of diagrams 7(a'), 7(b'), 7(c'), $\cdots$ [which are, for example, the left-hand parts of the sequence 7(a), 7(b), 7(c), $\cdots$]. If it were not for the (two) propagator lines at the bottom, the sum of this set would yield the compensation condition and thus be zero. But the extra propagator lines affect the value of the diagram only when intermediate states are involved, as in 7(c'), 7(d'), $\cdots$. Thus the difference between the sum of the primed and the compensation sets is of second order.

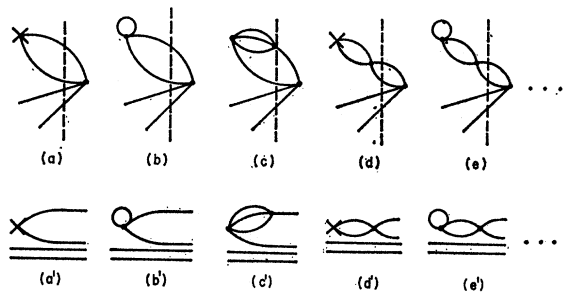

FIG. 7. Diagrams (a), (b), (c), (d), $\cdots$ are a subset of vacuum-to-pair diagrams. The pieces to left of the broken lines are explicitly displayed in diagrams (a'), (b'), (c'), (d'), $\cdots$. It is shown in the text that the sum of diagrams (a'), (b'), (c'), (d') are of second order, and hence the sum of (a), (b), (c), (d), $\cdots$ are of third order.

1. Renormalized Particle Energies, $\hat{\epsilon}_{\mathbf{k}}$.

In Fig. 8 are displayed some of the types of diagrams which contribute to $\hat{\epsilon}_{\mathbf{k}}$. The particular set displayed is the beginning of a sequence which, when summed, gives [compare Eq. (2.10)]

$$\epsilon_1+\sum_{1'}v_{1'}^2\langle 1\,1'|T(\xi_1+\xi_{1'})|1\,1'\rangle, \tag{2.15}$$

with the T matrix satisfying

$$\begin{aligned}&\langle 1'2'|T(\omega)|1\,2\rangle\\&=\langle 1'2'|V|1\,2\rangle+\sum_{1''2''}\langle 1'2'|V|1''2''\rangle\\&\quad\times\frac{u_{1''}^2u_{2''}^2\delta_{1''+2'',1+2}}{-\omega-(\xi_{1''}+\xi_{2''})}\langle 1''2''|T(\omega)|1\,2\rangle.\end{aligned} \tag{2.16}$$

This corresponds closely to the Brueckner T matrix for summing particle-particle scattering in the presence of a pair of holes of momentum $(-1, -1')$—the major diagrams which are summed in the elementary Brueckner theory—the only difference being that in the latter case the u's are given by the normal transformation (2.6).

In Fig. 8(b) is shown a set of diagrams for calculating the renormalized energy of a single "particle." The diagrams in 8(b) have exactly the same topological structure as 8(a), but differ in the intermediate propagators which enter in second order and beyond. We will not here be concerned with the actual calculation of $\hat{\epsilon}_{\mathbf{k}}$, but will rather rely for these upon previous calculations on

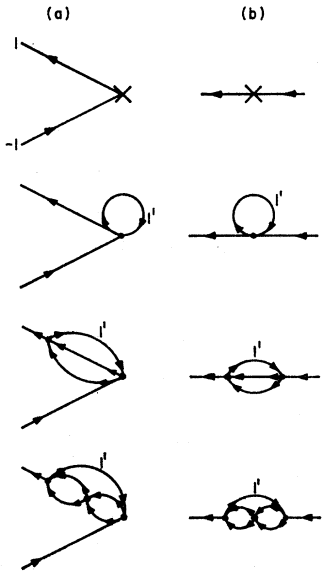

FIG. 8. A comparison of diagrams (a) contributing to $\hat{\epsilon}$, with a topologically equivalent set (b) contributing to the renormalized single "particle" energy.

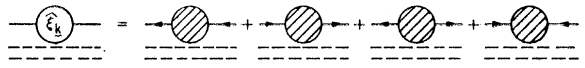

FIG. 9. Contributions to the renormalized single quasiparticle propagator $\hat{\xi}_k$.

the "normal" state of nuclear matter. This is predicated on the assumption that $\hat{\epsilon}_k$ depends only weakly on Δ_k when Δ_k is small. In calculations reported here, we further assume that $\hat{\epsilon}_k$ can be described by an effective-mass approximation

$$\hat{\epsilon}_k \approx (k^2 - k_F^2)\hbar^2/2m^*, \tag{2.17}$$

where m^* is evaluated at the Fermi surface.

2. *Renormalized Quasiparticle Energies* $\hat{\xi}_k$

The energy denominators which enter into propagators for intermediate states are the sums of ξ's, which in lowest order are given by Eq. (2.8). The diagrams which determine the renormalized propagator energies, $\hat{\xi}_k$, are given in Fig. 9; the external u and v factors are here included in the sum. Through first order in the potential, these diagrams give the result in Eq. (2.13). When intermediate-state propagators enter into the evaluation of the blobs in Fig. 9, the diagrams also depend on these intermediate states (they are represented by dashed lines in Fig. 9), since these affect the energy denominators. We will make the independent quasiparticle approximation and take the $\hat{\xi}_k$ to be independent of the number of other excitations.[12] Consistent

FIG. 10. T-matrix-type vacuum-to-pair diagrams. These are not allowed.

with this approximation, we will evaluate the internal factors of the blobs in Fig. 9 by bending the right-hand legs around and equating to the *topologically* equivalent diagrams in Fig. 6 (i.e., the compensation condition). This gives

$$\hat{\xi}_k = (u_k^2 - v_k^2)\hat{\epsilon}_k - u_k v_k \sum_{k'} u_{k'} v_{k'} G_{kk'}$$
$$= (\Delta_k^2 + \hat{\epsilon}_k^2)^{1/2}. \tag{2.18}$$

Equations (2.11) and (2.14) were used in obtaining the final form. Note that this is formally identical with Eq. (2.13).

3. *Renormalized Pairing Potential* $G_{kk'}$

The remainder of this paper is primarily devoted to the evaluation of $G_{kk'}$ and the subsequent effect on the nuclear energy gap. We note first, that G is *not* related to the Brueckner T matrix. Replacement of G by T would sum diagrams of the type shown in Fig. 10, but these contain intermediate states consisting of only an isolated pair, and must be excluded. In different terminology, including the diagrams of Fig. 10 would result in double counting.

The kinds of diagrams we will consider are displayed in Fig. 11. Diagrams with all arrows reversed and topologically equivalent variations of such diagrams must also be included. Not all of the diagrams shown will be summed simultaneously. We note, in particular, that (b′) contains two extra (a total of three) factors of $u_q v_q = \Delta_q/2(\Delta_q^2 + \hat{\epsilon}_q^2)^{1/2}$, and is expected to be considerably smaller than diagrams with only one such factor. We have not obtained an analytic estimate of the reduction of diagrams due to factors of uv, but in Sec. IV a numerical comparison is made. It is plausible[10] that each function uv reduces a diagram by a factor proportional to Δ.

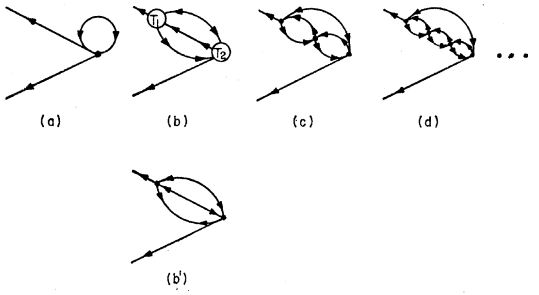

FIG. 11. Some diagrams which contribute to the renormalized pairing interaction. In diagram (b), the potential vertices have been replaced by T matrices, see Fig. 12.

For some simple potentials, it is possible to sum special infinite sets of diagrams. In the case of nuclear potentials which contain repulsive infinite cores, it is necessary to sum some subset (if one goes beyond the BCS approximation) in order to obtain finite results. Thus in Fig. 11(b) the two potential vertices have been replaced by T matrices (T_1 and T_2). These T matrices are sums of diagrams which involve pairs of lines with arrows pointing only to the left ("forward-going

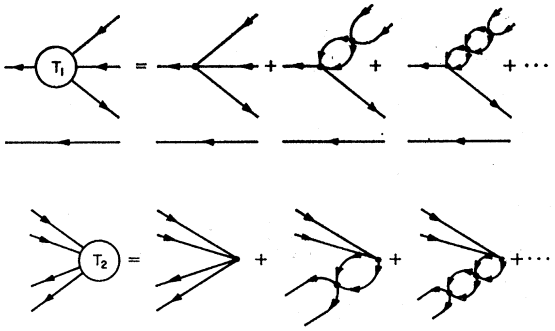

FIG. 12. Diagrammatic representation of the T matrices of Fig. 11(b). Only interactions of bubbles with arrows pointing to the left are included.

[12] See, however, H. A. Bethe, B. H. Brandow, and A. G. Petschek, Phys. Rev. **129**, 225 (1963).

graphs"), as indicated in Fig. 12:

$$\langle 1'2'|T_1|1\,2\rangle=\langle 1'2'|T(\hat{\xi}_{1'}+\hat{\xi}_{2'})|1\,2\rangle,$$
$$\langle 1'2'|T_2|1\,2\rangle=\langle 1'2'|T(\hat{\xi}_1+\hat{\xi}_2)|1\,2\rangle, \quad (2.19)$$

and $T(\omega)$ is given by Eq. (2.16). [When variations of (b) are included, only the T matrices derived from forward-going graphs are considered.] The limit $\Delta\to 0$ [i.e., replacing the u's by the normal distribution function Eq. (2.6)] is well defined in Eq. (2.16) and should introduce no new singularities. Depending upon the particular potential employed, $T(\omega)$ may or may not have a pole in the range of interest, i.e., $\omega>2\Delta$. For a purely attractive potential, such a pole always exists (at least for $\mathbf{k}_1+\mathbf{k}_2=0$) and is located at exactly minus the energy of the Cooper pair state.[13] It can be shown (Sec. III) for a separable attractive interaction that the pole lies below $2\Delta^{(0)}$, where $\Delta^{(0)}$ is the gap calculated to lowest order [i.e., using Eq. (2.11)]. In the case of the particular nuclear potentials employed, we have established that there is no pole for the singlet interaction. The triplet interaction—which has a pole at the deuteron binding energy when $k_F=0$—has a pole in ω very close to zero, and positive. This is an annoying accident and can be circumvented either by decreasing the attraction slightly or by assuming the existence of a small but finite gap. We chose the latter.

The sequence diagrams of Fig. 11(a), (b) (with T replaced by V), (c), (d), $\cdots$, can be summed for some special interactions that are discussed in Sec. III. In that case, the pairing interaction $G_{\mathbf{k}\mathbf{k}'}$ can be written as the sum

$$G_{\mathbf{k}\mathbf{k}'}{}^0[1-f\gamma_{kk'}+(f\gamma_{kk'})^2-\cdots]=\frac{G_{\mathbf{k}\mathbf{k}'}{}^0}{1+f\gamma_{kk'}}.$$

If the contribution of (b) is small compared to that of (a), this justifies terminating the sequence with (b). Its contribution to the effective pairing interaction is[9]

$$G_{k_1k_2}{}^b=2\sum_{s_2t_2}\sum_{3\,4}u_3{}^2v_4{}^2 \times\frac{\langle -1\,4|V|-3\,2\rangle\langle -3\,1|V|-2\,4\rangle}{\hat{\xi}_1+\hat{\xi}_2+\hat{\xi}_3+\hat{\xi}_4}. \quad (2.20)$$

The diagrams for the renormalized pairing potential also have an analogy with conventional perturbation theory. Thus, corresponding to Fig. 11, we find the diagrams of Fig. 13 (and similar diagrams with reversed arrows, etc.) which are obtained by breaking the leg with opposite arrows in Fig. 11. [There is no perturbation diagram corresponding to 11(b').] The diagrams 13(b), 13(c), 13(d), $\cdots$, in perturbation language, contain the exchange of particle-hole pairs.

4. *Isotropy of* $\Delta_{\mathbf{k}}$

Although nuclear matter by definition has rotational symmetry, it is not obvious that the solutions of the generalized integral equation (2.14) also possess rotational symmetry. The question already arises in lowest order ($G=V$) when the potential contains components beyond the s wave,[14] and occurs for the general G even when only s-wave scattering is considered. The pairing interaction is capable of polarizing the medium in a preferred direction. (Such phenomena are familiar in crystalline structure.) The energy levels of the system are degenerate with respect to the orientation of the preferred direction. This degeneracy can be utilized to generate another state which has an isotropic spectrum —namely, a linear combination of state vectors which is in average over all directions of orientation.

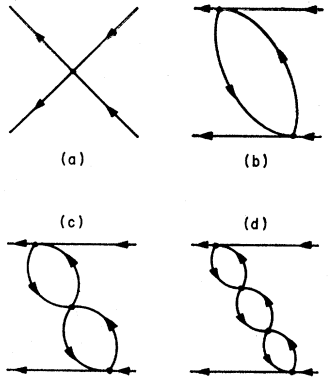

FIG. 13. Conventional perturbation analog of Fig. 11; these diagrams contribute to the renormalized pairing interaction. Note change of both horizontal and vertical scales at $k=3F^{-1}$.

The anisotropy effects are real and interesting, but will be ignored in the present analysis; that is, we take $\Delta_{\mathbf{k}}$ to be isotropic. This immediately allows us to average $G_{\mathbf{k}\mathbf{k}'}$ over the angles between $\mathbf{k}$ and $\mathbf{k}'$. The resultant average depends only on the magnitudes of $\mathbf{k}$ and $\mathbf{k}'$ and is denoted by $G_{kk'}$.

III. ONE-DIMENSIONAL PROBLEM

A. Through Second Order

In order to gain some insight into the importance of higher order corrections to the BCS equation, we first investigate the one-dimensional problem for one type of Fermion interacting solely in singlet s states:

$$\langle 3\,4|V|1\,2\rangle=\langle k_3k_4|V|k_1k_2\rangle \times\delta(k_3+k_4-k_1-k_2)S(3\,4)S(1\,2), \quad (3.1)$$

where

$$S(1\,2)=\delta_{s_1,1/2}\delta_{s_2,1/2}-\delta_{s_1,-1/2}\delta_{s_2,1/2}.$$

For simplicity, we have studied an attractive "shell" interaction[15] ($\hbar=2m=1$)

$$\langle k_3k_4|V|k_1k_2\rangle=-f \quad \text{for} \quad (|k_i|-k_F)^2<w, \quad i=1,2,3,4,$$
$$=0 \quad \text{otherwise}, \quad (3.2)$$

[13] L. N. Cooper, Phys. Rev. **104**, 367 (1956).

[14] K. A. Brueckner, T. Soda, P. W. Anderson, and P. Morel, Phys. Rev. **118**, 1442 (1960); R. Balian and N. R. Werthamer, *ibid.* **131**, 1553 (1963).

[15] The specific form of the potential is not crucial so long as it is a smoothly varying function. Thus, we have also investigated the problem for a separable Yamaguchi potential and have obtained similar results.

with $w \ll k_F^2$. The integral equation for Δ_k through second order is

$$\Delta_k = \tfrac{1}{2} f \sum_{k'} \frac{\Delta_{k'}}{\hat{\xi}_{k'}} \times \left[1 - 2f \sum_q \frac{u_{k+q}^2 v_{k'-q}^2 - (uv)_{k+q}(uv)_{k'-q}}{\hat{\xi}_k + \hat{\xi}_{k'} + \hat{\xi}_{k+q} + \hat{\xi}_{k'-q}} \right]. \quad (3.3)$$

Because of the form of the potential (3.2), the sums are restricted so that the momenta k, k', $k+q$, and $k'-q$ all lie within the shell. We use the effective-mass approximation for the energies $\hat{\epsilon}_k = (k^2 - k_F^2)m/m^*$.

The solution of the lowest order integral equation (only first-order terms in f are kept) yields a gap which is constant inside the shell region:

$$\Delta_k{}^0 = \Delta^0 = \frac{2k_F w m}{m^* \sinh(1/g)} \xrightarrow[g \gg 1]{} \frac{4k_F w m}{m^*} e^{-1/g}, \quad (|k| - k_F)^2 < w,$$
$$= 0 \quad \text{otherwise}, \quad (3.4)$$

where

$$g = fm^*/(2\pi m k_F).$$

We now turn to the solution of (3.3) including the second-order terms. In particular, we solve for $\Delta = \Delta_{k_F}$ with the assumption that on the right-hand side of (3.3) the momentum dependence of $\Delta_{k'}$ can be neglected inside the shell region. This is a good approximation, since $\Delta_{k'}$ is important only near the Fermi surface. Moreover, we have seen that Δ_k is independent of k for the leading order solution (3.4). The effect of the second-order terms in f is to cause Δ_k to be an increasing function of $||k| - k_F|$. This is because the u^2v^2 term dominates the $(uv)(uv)$ term, and the major k dependence arises from the energy denominator. This yields the result that the second-order term is an algebraically increasing function of $||k| - k_F|$. Thus evaluating Δ_k at k_F underestimates the correction terms.

Consistent with the evaluation of the correction terms to second order, we will take the normal distributions (2.6) for u and v and, in the energy denominator of the second-order term, set

$$\hat{\xi}_k = 2k_F ||k| - k_F| / (m^*/m).$$

The integrals can now be evaluated. The leading order expression for (3.3) when the gap is small (i.e., $fm^*/2\pi m k_F = g \ll 1$), is

$$1 = F(1 - \tfrac{1}{4}F) + O(g), \quad (3.5a)$$

where

$$F = g \ln(2k_F m w / m^* \Delta). \quad (3.5b)$$

The terms $O(g)$, which we now neglect, include the contribution of the $(uv)(uv)$ term. Note that the dominant second-order terms are comparable with the first-order terms and are not of order $e^{-1/g}$ as suggested by Bogoliubov, Tolmachev, and Shirkov.[10]

The lowest order solution obtains from setting $F = 1$. The solution of (3.5) requires $F = 2$, or

$$\Delta \approx (4k_F m/m^*) e^{-2/g}, \quad g \ll 1. \quad (3.6)$$

Equation (3.6) differs from (3.4) in that $e^{-1/g}$ is now replaced by $e^{-2/g}$. This is, of course, a very large reduction for $g \ll 1$. Note that if the terms $O(g)$ are negative, no solution obtains.

B. Sum of "Particle-Hole" Graphs

Because of the importance of the second-order corrections, it is of interest to investigate higher order terms. Since our potential is separable in each momentum coordinate, the sum of diagrams (a), (b) [with $T_1 = T_2 = V$], (c), (d), $\cdots$, in Fig. 11 can be written explicitly as

$$G_{kk'} = -f[1 - \gamma_{kk'} + (\gamma_{kk'})^2 - (\gamma_{kk'})^3 + \cdots] = \frac{-f}{1 + \gamma_{kk'}}, \quad (3.7)$$

with

$$\gamma_{kk'} = 2f \sum_q \frac{u_{k+q}^2 v_{k'-q}^2}{\hat{\xi}_k + \hat{\xi}_{k'} + \hat{\xi}_{k+q} + \hat{\xi}_{k'-q}}. \quad (3.8)$$

Note that $\gamma_{kk'}$ is positive for an attractive interaction, and tends to weaken the strength of G relative to the lowest order value.[16] In particular, we note that

$$\gamma_{k_F k_F} \approx \tfrac{1}{4} g \ln \frac{2k_F w m}{m^* \Delta} = \tfrac{1}{4} F, \quad g \ll 1. \quad (3.9)$$

If we replace $G_{kk'}$ by $G_{k_F k_F}$ and $\Delta_{k'}$ by Δ in the integral equation (2.14) we obtain, instead of (3.5),

$$1 = F/(1 + \tfrac{1}{4}F), \quad (3.10)$$

or $F = \frac{4}{3}$, and for the gap parameter

$$\Delta \approx (4k_F m/m^*) e^{-4/3g}. \quad (3.11)$$

There is still a significant reduction in the gap relative to lowest order value (3.4), but it is not so dramatic as the second-order result (3.6).

The same method of summing "particle-hole" diagrams can be extended trivially to three dimensions for the "shell" interaction or the exchange part of a local interaction. If the second-order term is already small compared with the leading order term, however, we are justified in terminating the sequence at second order.

C. T-Matrix Vertices

We now investigate the effect of employing T matrices in diagram (b) of Fig. 11. The T-matrix integral

[16] For a repulsive interaction, G may have a pole corresponding to a collective "exciton"; A. Bardasis and J. R. Schrieffer, Phys. Rev. **121**, 1050 (1961).

equation (2.16) can be solved to yield

$$\langle p+k, p-k|T(\omega)|p+k', p-k'\rangle = \frac{-f}{1-f\sum_q u_{p+q}{}^2 u_{p-q}{}^2/(\omega+\hat{\xi}_{p+q}+\hat{\xi}_{p-q})}, \quad (3.12)$$

where it is understood that all momenta lie within the shell region.

The question arises whether (and where) $T(\omega)$ has a pole corresponding to a Cooper pair state. This has been investigated by Tomasini,[17] who has shown in a perturbation context, that no such pole can exist. The argument must be modified in our self-consistent treatment.[18] The term $\sum_q$ in the denominator is largest when $p=0$ and $\omega=2\Delta$ (the smallest value ω assumes). In this case

$$\langle k-k|T(2\Delta)|k'-k'\rangle = \frac{-f}{1-\frac{1}{2}f\sum_q u_q{}^4/(\Delta+\hat{\xi}_q)} \equiv \frac{1}{1-h(\Delta)}, \quad (3.13)$$

and a pole arises if h can equal unity. But $h(\Delta)$ satisfies the inequalities

$$h(\Delta)=\tfrac{1}{2}f\sum_q \frac{u_q{}^4}{\Delta+\hat{\xi}_q}<\tfrac{1}{2}f\sum_q \frac{u_q{}^4}{\hat{\xi}_q}<\tfrac{1}{4}f\sum_q \frac{1}{\hat{\xi}_q}. \quad (3.14)$$

In the limit of $g\ll 1$ and $\Delta/w^{1/2}k_F\ll 1$, the inequalities approach equalities, and we find

$$h(\Delta)\to\tfrac{1}{2}F(\Delta). \quad (3.15)$$

Thus, if the lowest order BCS integral equation is used to determine Δ, we note that $h(\Delta^0)\to\frac{1}{2}$, and no pole occurs.[17] However, we have seen that the inclusion of particle-hole scattering [Eq. (3.7)] tends to decrease the energy gap. If only second-order diagrams are included, $h(\Delta)\to 1$, but if the whole set of particle-hole diagrams is summed (see Fig. 11), $h(\Delta)\to\frac{2}{3}$.

The effect of replacing V by T, as in Fig. 11(b), is to increase the second-order correction (when V is attractive), decrease the gap, and hence increase h beyond the value $\frac{2}{3}$. Perhaps, a crude estimate of this replacement can be obtained by inserting T at every vertex in Figs. 11(b), (c), $\cdots$ [not (a)]; that is, f is replaced by $f/(1-h)\approx f/(1-\frac{1}{2}F)$. Then Eq. (3.10) becomes

$$1=\frac{F}{1+\frac{1}{4}F/(1-\frac{1}{2}F)}, \quad (3.16)$$

which has no solution for F real. This is undoubtedly too stringent a bound, since the T matrix assumes the value $-f/(1-\frac{1}{2}F)$ only at one point [$p=0$, $\omega=2\Delta$ in Eq. (3.12)] and we must integrate T over a range of values of p and ω. Hence, no definite conclusion can be drawn about the existence of a pole of the T matrix, nor about the energy gap for the chosen interaction.

[17] A. Tomasini, Nuovo Cimento **20**, 963 (1961).
[18] See also Ref. 9.

IV. THREE-DIMENSIONAL PROBLEM

The results obtained in the previous section tell us that, in one dimension, higher order terms in the interaction cannot be neglected in solving for the energy gap. In a letter,[9] we have shown that this is not peculiar to the one-dimensional problem. For various attractive interactions acting only in singlet states, it was demonstrated that:

(a) The second-order interaction terms, $G^b+G^{b'}$, are not of order Δ compared with G^0 and they tend to reduce the energy gap.

(b) The $(uv)(uv)$ terms are small compared with the $(u^2)(v^2)$ terms if Δ is small.

(c) For some parameters of the interaction, there is no solution to the gap equation (2.14) when terms only up to second order in the interaction are included.

(d) It is necessary to solve the energy-gap equation self-consistently rather than resorting to a perturbation procedure. The latter arises in the evaluation of $\hat{\xi}(k_F)$ by standard perturbation methods following (say) a lowest order transformation characterized by Δ^0. Through second order, $\hat{\xi}(k_F)=\Delta$ is given by the right-hand side of Eq. (2.14). Perturbation theory would replace Δ by Δ^0 wherever it appears; the self-consistent procedure maintains Δ on the right-hand side. We rewrite the gap equation (2.14) in the form[9]

$$\Delta=fI_1(\Delta)-f^2I_2(\Delta), \quad (4.1)$$

where $-f$ is the strength of the interaction. In the limit of small Δ, $I_2(\Delta)/I_1(\Delta)$ approaches a constant independent of Δ, in contrast to the one-dimensional case [see Eq. (3.5)]. To illustrate the difference between the self-consistent and perturbation solutions of (4.1), we note that for sufficiently small gaps, we may set

$$\begin{aligned} I_1&=c_1\ln(\beta/\Delta), \\ I_2&=c_2\ln(\beta/\Delta), \end{aligned} \quad (4.2)$$

where c_1 and c_2 are constants and β is some characteristic range of the interaction. The self-consistent solution of (4.1) is

$$\Delta=\Delta^0\exp\left[\frac{-c_2}{c_1{}^2(1-fc_2/c_1)}\right]\simeq\Delta^0\exp(-c_2/c_1{}^2), \quad (4.3)$$

where $\Delta^0=\beta e^{-1/(fc_1)}$ and the final form assumes $fc_2/c_1\ll 1$. On the other hand, the perturbation solution yields

$$\Delta_{\rm pert}=\Delta^0\left[1-\frac{c_2}{c_1{}^2}(fc_1)\right]. \quad (4.4)$$

If $c_2/c_1{}^2$ is numerically small, for example, we find

$$\frac{\Delta_{\rm pert}-\Delta^0}{\Delta-\Delta^0}=fc_1. \quad (4.5)$$

Thus the perturbation procedure would predict a much smaller correction to the energy gap than would the self-consistent procedure. We wish to emphasize that the differences do not approach each other even when the corrections are small.

We have not summed particle-hole graphs in the three-dimensional case, but as indicated in the letter,[9] this can be done for the exchange part of a separable interaction.

V. NUCLEAR MATTER

With the insights gained from our studies in Secs. III and IV, we now investigate the energy gap in infinite nuclear matter. For small gaps, we have seen that the contribution to $G_{kk'}$ given by diagram 11(b') is small compared with that of (b). Furthermore, if G^b is small compared with G^0, as is found to be the case, then it is consistent to neglect diagrams 11(c), (d), $\cdots$. Thus we only investigate G^b. Whereas in lowest order only the singlet component of the interaction contributes to G^0, both singlet and triplet components contribute to G^b. We note also that the particle-hole pair exchanged between the vertices can be either a neutron pair or a proton pair regardless of the isospin of the external lines.

The sum of all diagrams of the type 11(b) leads to the contribution ($\hbar^2=2m=1$)

$$G^b=(5/4)G^{ss}-\tfrac{3}{4}(G^{st}+G^{ts}+G^{tt}), \tag{5.1}$$

where

$$G_{kk'}{}^{\nu\nu'}=2\sum_{\mathbf{q}}\frac{u_{\mathbf{k}+\mathbf{q}}{}^2v_{\mathbf{k}'-\mathbf{q}}{}^2}{\hat{\xi}_{\mathbf{k}}+\hat{\xi}_{\mathbf{k}'}+\hat{\xi}_{\mathbf{k}+\mathbf{q}}+\hat{\xi}_{\mathbf{k}'-\mathbf{q}}}$$
$$\times\langle-\mathbf{k},\mathbf{k}'-\mathbf{q}|\,T^{\nu}(\hat{\xi}_{\mathbf{k}}+\hat{\xi}_{\mathbf{k}'-\mathbf{q}})\,|-\mathbf{k}-\mathbf{q},\mathbf{k}'\rangle$$
$$\times\langle-\mathbf{k}-\mathbf{q},\mathbf{k}|\,T^{\nu'}(\hat{\xi}_{\mathbf{k}'}+\hat{\xi}_{\mathbf{k}'-\mathbf{q}})\,|-\mathbf{k}',\mathbf{k}'-\mathbf{q}\rangle,$$
$$[\nu,\nu'=s(\text{singlet}),\ t(\text{triplet})]. \tag{5.2}$$

The T matrices satisfy the equations [compare (2.16)]

$$\langle\mathbf{p}+\mathbf{k}',\mathbf{p}-\mathbf{k}'|\,T^{\nu}(\omega)\,|\mathbf{p}+\mathbf{k},\mathbf{p}-\mathbf{k}\rangle$$
$$=\langle\mathbf{p}+\mathbf{k}',\mathbf{p}-\mathbf{k}'|\,V^{\nu}\,|\mathbf{p}+\mathbf{k},\mathbf{p}-\mathbf{k}\rangle$$
$$-\sum_{\mathbf{k}''}\frac{u_{\mathbf{p}+\mathbf{k}''}{}^2u_{\mathbf{p}-\mathbf{k}''}{}^2}{\omega+\hat{\xi}_{\mathbf{p}+\mathbf{k}''}+\hat{\xi}_{\mathbf{p}-\mathbf{k}''}}$$
$$\times\langle\mathbf{p}+\mathbf{k}',\mathbf{p}-\mathbf{k}'|\,V^{\nu}\,|\mathbf{p}+\mathbf{k}'',\mathbf{p}-\mathbf{k}''\rangle$$
$$\times\langle\mathbf{p}+\mathbf{k}'',\mathbf{p}-\mathbf{k}''|\,T^{\nu}(\omega)\,|\mathbf{p}+\mathbf{k},\mathbf{p}-\mathbf{k}\rangle. \tag{5.3}$$

The T matrix was evaluated using the normal [Eq. (2.6)] form for the u's and replaclng $\hat{\xi}$ by $|\hat{\epsilon}|$. The potentials employed were of the Puff type; that is, the s-wave part of a hard shell plus an attractive Yamaguchi:

$$\langle\mathbf{p}+\mathbf{k}',\mathbf{p}-\mathbf{k}'|\,V^{\nu}\,|\mathbf{p}+\mathbf{k},\mathbf{p}-\mathbf{k}\rangle$$
$$=\lim_{\lambda_c\to\infty}\lambda_c\frac{\sin k'r_c}{k'}\frac{\sin kr_c}{k}-\frac{2(2\pi)^3\lambda_{\nu}}{(\beta_{\nu}{}^2+k'^2)(\beta_{\nu}{}^2+k^2)}. \tag{5.4}$$

The T matrix for a potential which can be written as a finite sum of separable terms,

$$\langle\tfrac{1}{2}\mathbf{K}+\mathbf{p},\tfrac{1}{2}\mathbf{K}-\mathbf{p}|\,V\,|\tfrac{1}{2}\mathbf{K}'+\mathbf{p}',\tfrac{1}{2}\mathbf{K}'-\mathbf{p}'\rangle$$
$$=\delta(\mathbf{K}-\mathbf{K}')(2\pi)^3\sum_{\alpha}\lambda_{\alpha}w_{\alpha}(p)w_{\alpha}(p')$$

can be written

$$\langle\tfrac{1}{2}\mathbf{K}+\mathbf{p},\tfrac{1}{2}\mathbf{K}-\mathbf{p}|\,T(\omega)\,|\tfrac{1}{2}\mathbf{K}'+\mathbf{p},\tfrac{1}{2}\mathbf{K}'-\mathbf{p}'\rangle$$
$$=\delta(\mathbf{K}-\mathbf{K}')\sum_{\alpha\alpha'}([\mathbf{\Lambda}+\mathbf{L}(K,\omega)]^{-1})_{\alpha\alpha'}w_{\alpha}(p)w_{\alpha'}(p'),$$

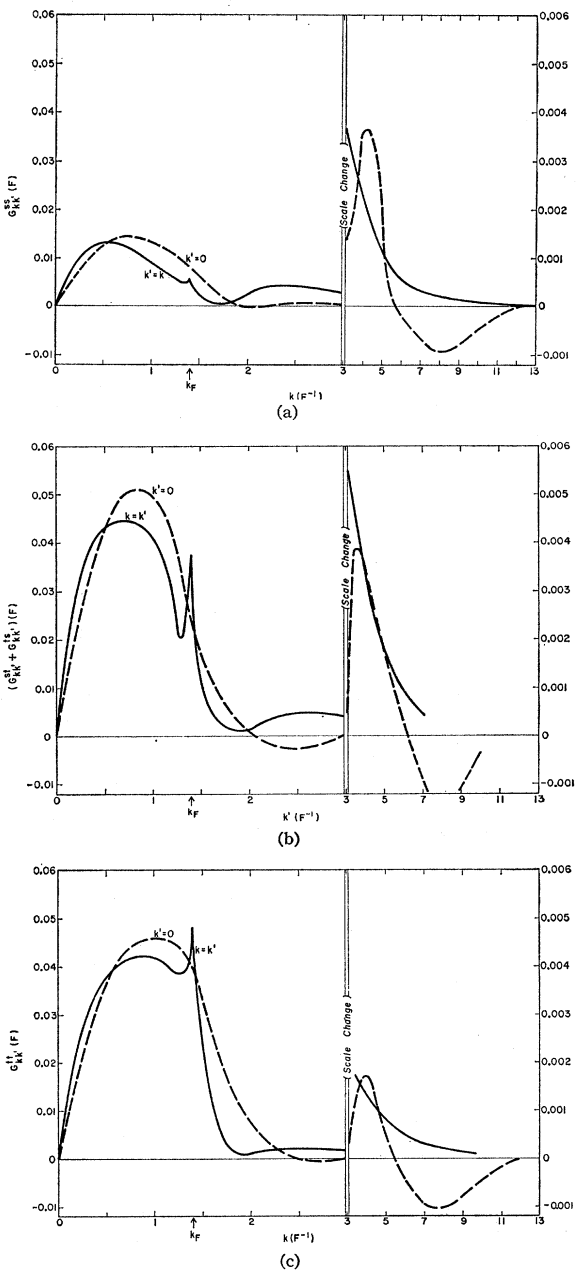

FIG. 14. Plots of the contributions to $G_{kk'}{}^b$ along the cuts $k'=0$ and $k'=k$. Here $m^*/m=1$.

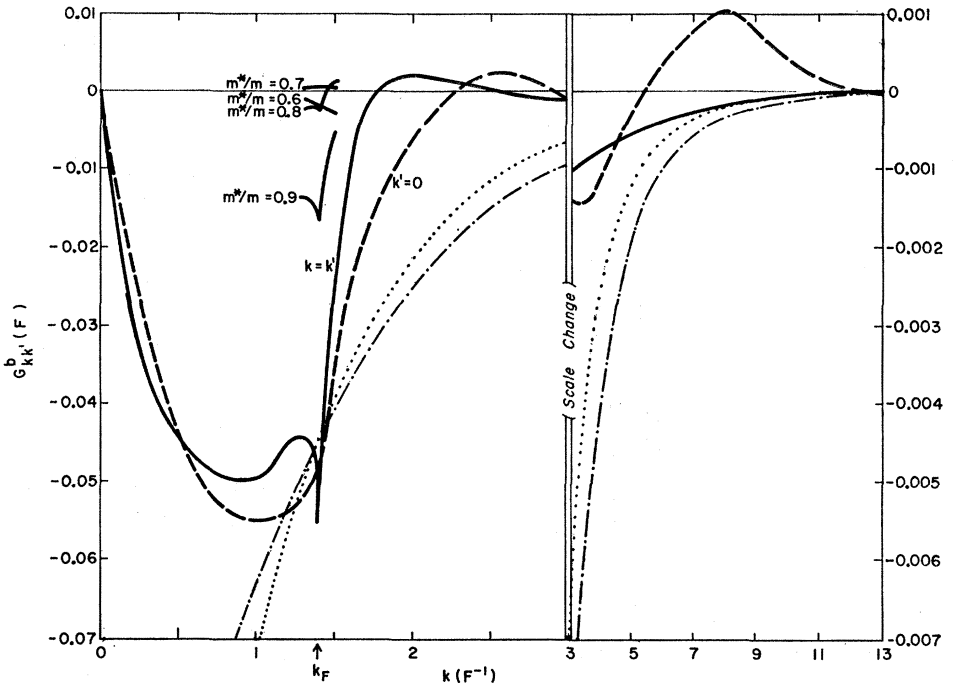

FIG. 15. Plot of $G_{kk'}{}^b$ for $k'=0$ and $k'=k$. The complete solid and dashed curves are for $m^*/m=1$. Fragments of curves for $k=k'$ close to k_F are shown for various values of m^*/m. The dotted curve and the dot-dash curve are Yamaguchi representations ($m^*/m=1$, $k'=k$) of $G_{kk'}{}^b$ corresponding to the two ranges of the interaction given in Table I. Note change of both horizontal and vertical scales at $k=3\mathrm{F}^{-1}$.

where $\mathbf{\Lambda}$ is a diagonal matrix with elements λ_α and the matrix elements of $\mathbf{L}(K,\omega)$ are given by

$$L_{\alpha\alpha'}=\lambda_\alpha\int d\mathbf{p}''\frac{w_\alpha(p'')u^2{}_{\mathrm{p}+\frac{1}{2}\mathrm{K}}u^2{}_{\mathrm{p}-\frac{1}{2}\mathrm{K}}w_{\alpha'}(p'')}{\omega+(\frac{1}{2}K^2+2p''^2)/(m^*/m)}.$$

These integrals were evaluated in part analytically and in part numerically.

The parameters for the singlet and triplet interactions are listed in Table I.

The most extensive calculations were carried out using the singlet parameters I (original Puff[19]), although we now believe set II gives a better representation of the two-body scattering data.[8] It turns out that G^{tt} dominates G^b for most values of $\mathbf{k}$ and $\mathbf{k}'$, so that the final results are somewhat insensitive to the singlet potential assumed.

Plots of the three $G_{kk'}{}^{\nu\nu'}$ appear in Figs. 14 and $G_{kk'}{}^b$ is shown in Fig. 15 [$G_{kk'}$ is $G_{\mathbf{kk}'}$ averaged over the angle $\angle(\mathbf{kk}')$]. All computations were made with type-I potentials, and were carried out by a numerical four-dimensional Monte Carlo integration.[20] In the limit $\Delta\to 0$, $G_{kk'}{}^b$ is everywhere finite and continuous. It does, however, possess infinite first derivatives at $k=k'=k_F$, and can be shown to behave like

$$G_{k,k_F+x}{}^b=G_{k_F+x,k_F+x}{}^b\propto \mathrm{const}-|x|\ln|x|,\quad |x|\ll k_F. \quad (5.5)$$

When Δ is small but finite, the cusp at the Fermi surface is smoothed out over a momentum range of the order of $m^*\Delta/2mk_F$. The numerical integrations reported here were made with $\Delta=0.01\mathrm{F}^{-2}$ ($0.2074m/m^*$ MeV), $k_F=1.4\mathrm{F}^{-1}$, so that the cusps appear as narrow peaks $\sim 0.003\mathrm{F}^{-1}$ wide. $G_{kk'}{}^{ss}$, $G_{kk'}{}^{tt}$ and $(G_{kk'}{}^{st}+G_{kk'}{}^{ts})$ individually and therefore $G_{kk'}{}^b$ are symmetric with respect to the exchange of k and k'. Except for the cusp at $k=k'=k_F$, the G's are smoothly varying functions of k and k'. We have only exhibited plots for cuts through the (k,k') plane corresponding to $k=k'$ and $k'=0$, although we have investigated the functions (especially $G_{kk'}{}^{ss}$) more thoroughly. For large values of k (i.e., $k\gg\beta$), $G_{kk'}{}^{\nu\nu'}$ is determined almost solely by the hard core of the potential, and is thus independent of ν and ν'.

Figures 14 and 15 show that G^{tt} and $(G^{st}+G^{ts})$ are generally of the same sign as G^{ss}. However, they appear with opposite signs in Eq. (5.1). Thus G^{ss} alone would tend to *reduce* the energy gap in nuclear matter whereas the combination tends to *increase* the gap.

The most extensive survey was made for $m^*/m=1$. However, in Fig. 15 we have also plotted a segment of the $G_{kk}{}^b$ curve near the Fermi surface for various m^*/m.

TABLE I. Table of s-wave potential parameters. Type-I parameters are those given by Puff (Ref. 19); type II are derived in paper II and yield a better fit to the singlet s-wave scattering data.

	Singlet			Triplet		
Type	$\lambda(\mathrm{F}^{-3})$	$\beta(\mathrm{F}^{-1})$	$r_c(\mathrm{F})$	$\lambda(\mathrm{F}^{-3})$	$\beta(\mathrm{F}^{-1})$	$r_c(\mathrm{F})$
I	3.64	2.004	0.45	8.695	2.453	0.45
II	0.886	1.602	0.257	8.695	2.453	0.45

[19] R. Puff, Ann. Phys. (N.Y.) **13**, 317 (1961).

[20] These integrals were carried out by performing a transformation which increased the sampling where v^2 is large.

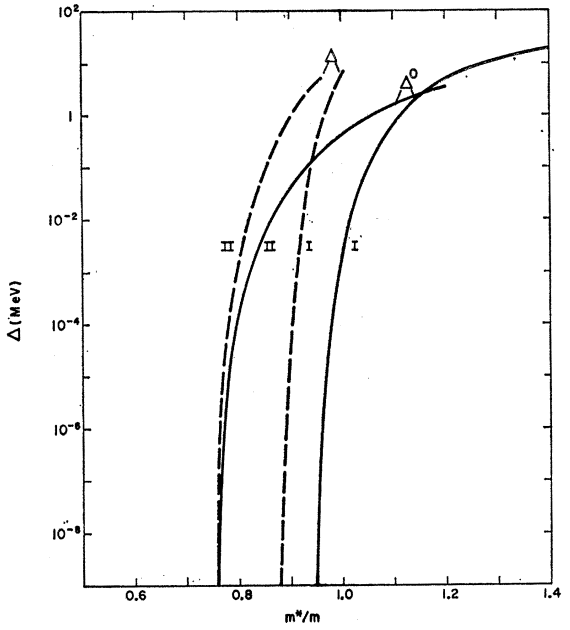

FIG. 16. Energy gap parameters Δ^0 and Δ as functions of m^*/m. The solid curves are calculated from the lowest order, BCS integral equation for the two potentials (types I and II) given in Table I (see also Ref. 8). The dashed curves include the contributions of $G_{kk'}{}^b$ calculated with the type-I potential.

It is seen that the numerical results are, unfortunately, extremely dependent upon the value of the effective mass. We say "unfortunately" because values of the effective mass which are sufficiently precise for our purposes are not available.

Generally, if the Hamiltonian is multiplied by the dimensionless effective mass m^*/m, then this parameter appears only multiplied by the potential—i.e., (energy $\times m^*/m$) is a function of (strength of the interaction $\times m^*/m$). When hard-shell interactions are present, then m^*/m appears only multiplied by the finite (attractive) part of the interaction (i.e., λ_ν).

The form $G_{kk'}{}^b$ in Fig. 15 shows that the potential falls off rapidly outside of the Fermi sphere. From the behavior of solutions to the BCS equation with shell interactions, we know that the strength of the potential (at the Fermi surface) enters into the argument of the exponential, whereas the momentum range of the interaction enters only multiplicatively. This suggests approximating G^b by some mathematically convenient potential of appropriate range. We have chosen a Yamaguchi potential of the same range as the attractive part of the singlet s-wave interaction. Once this approximation has been made, we can immediately utilize the calculations of paper II to estimate the energy gap, since $G=G^0+G^b$ now corresponds to a change in strength of the attraction (or of m^*). We have included in Fig. 15 the two Yamaguchi fits to $G_{kk}{}^b$ corresponding to the ranges of the attractive singlet parts of type-I and type-II potentials. (We "conservatively" chose the normalization to pass, not through $k=k'=k_F$, but, rather arbitrarily, through an average of the points at $k=k'=1.3$, 1.4, and 1.5. The point at $k_F=1.4$ was given double weight.) It is seen that G^b is of shorter range in k (longer range in configuration space) than the attractive singlet part of the nuclear potentials.

The solid curves[8] in Fig. 16 give the energy gap Δ^0 as a function of $m^*(k_F=1.4\text{F}^{-1})$ for the two potentials (see Table I). Associated with each solid curve is a broken curve for Δ obtained according to the prescription of the previous paragraphs. Recall that G^b is calculated using the type-I potential. We now believe that the type-II potential is a better fit to the singlet scattering data. The triplet interaction is more important than the singlet in determining G^b (compare Fig. 14), but G^0 is determined completely by the singlet interaction. This tends to lend somewhat more credence to the type II results in Fig. 16. From this figure we note that unless m^*/m is larger than 0.85, the energy-gap parameter in nuclear matter remains uninterestingly less than 0.1 MeV. Nevertheless, the higher order corrections computed here are seen to have a large effect on the magnitude of the gap. (Note that the difference between the results for two potentials is relatively less important when the gap is large.) The value of m^*/m suggested by Brueckner *et al.*[21] is 0.73. Bethe, Brandow, and Petschek[12] estimate an effective mass of 0.85 for the reference spectrum; the relevance of the reference spectrum will be examined in the next section.

VI. CONCLUSIONS

In an accompanying paper[8] it is shown that for "realistic" forces the BCS energy gap in nuclear matter is several orders of magnitude lower than that deduced for the heaviest nuclei. In this article we have attempted to improve the nuclear-matter calculations by generalizing the gap equation to include higher order terms in the transformed interaction. Both here and in a previous Letter,[9] we have conclusively demonstrated that such higher order terms which allow nontime-reversed pairs to be scattered, are not negligible, as had been argued.[10] Their inclusion can change the numerical value of the gap in nuclear matter by orders of magnitude. The computed value of the gap is sensitive to the effective mass and to details of the nuclear potential in the range where the gap is small and therefore uninteresting. However, it becomes less sensitive to these parameters as the gap increases. Qualitatively we can say that if the effective mass is less than about 0.75, the gap parameter Δ is expected to be negligible; if the effective mass is larger than about 0.85, then we expect Δ to be larger than $\sim$0.1 MeV.

In order to improve upon the reliability of the above calculation, we might suggest the following:

(a) One should include the difference between the energy spectrum of intermediate states that occur in

[21] K. A. Brueckner, J. L. Gammel, and J. T. Kubis, Phys. Rev. 118, 1438 (1960).

higher order diagrams and that of an isolated quasiparticle. The $\hat{e}_k$ which enters in $\hat{\xi}_k=(\Delta_k^2+\hat{e}_k^2)^{1/2}$ is closely related to the normal single-particle energy computed by Brueckner *et al.*[21] ($m^*/m\sim0.7$), but the intermediate-state energies [which enter both in the T-matrix series and explicitly in the integral for G^b, Eq. (5.2)] are more closely related to the reference spectrum of Bethe, Brandow, and Petschek. The reference spectrum energies are characterized by a larger effective mass ($m^*\sim0.85$) and an additive constant.

(b) It would be useful to repeat our calculations with the best phenomenological potentials (with explicit use of one-pion exchange), thus including the effects of relative angular-momentum states beyond $l=0$. In that case it would also be interesting to determine the anisotropy of the gap with respect to some arbitrary direction.

The results of our calculation lead us to believe that the energy gap in infinite nuclear matter is very small, if not absent. This suggests that the gap may well be a finite-size effect, and work is in progress to determine whether this is indeed the case.

ACKNOWLEDGMENTS

The authors are grateful to Dr. B. A. Jacobsohn, Dr. A. Bohr, Dr. B. R. Mottelson, and Dr. D. Falk for illuminating discussions and comments. They wish to thank J. Hartle, R. Kennedy, and W. Shaw for valuable assistance in various phases of the numerical computations.

PHYSICAL REVIEW VOLUME 133, NUMBER 5B 9 MARCH 1964

Energy Gap in Nuclear Matter. II. BCS Theory*

R. KENNEDY, L. WILETS, AND E. M. HENLEY
University of Washington, Seattle, Washington
(Received 10 October 1963)

The Bardeen-Cooper-Schrieffer (BCS) theory is employed to study the energy gap in nuclear matter with various internucleonic potentials which fit singlet low-energy scattering data and the s-wave phase shift at 310 MeV. The interactions are expressed as the sum of two terms, each of which is separable, thus admitting exact solutions of the energy-gap equation. The dependence of the energy gap on the form and parameters of the interaction, as well as on the nuclear density and effective mass, is investigated. For normal nuclear density, the gap is found to be small compared with that observed in the heaviest nuclei.

I. INTRODUCTION

THE prediction of an energy gap in the spectrum of a superconductor by the theory of Bardeen, Cooper, and Schrieffer[1] (BCS) and observations on the spectra of even-even nuclei have led to the speculation that the same concepts might apply to nuclei[2] and nuclear matter.[3,4] An essential feature of a superconducting system is the attractive interaction of time-reversed pairs near the Fermi surface. The present paper uses this feature to study the energy gap in infinite nuclear matter.

Solutions of the basic integral equation are obtained which qualitatively confirm the results of Emery and Sessler,[5] who used a Gammel-Thaler potential acting in s waves only. In addition, we show the effects on the gap of different forms of the potential between nucleons, define criteria for the existence of an energy gap (see also Ref. 4), and compare approximate solutions with exact solutions of the integral equations.

II. ENERGY GAP FOR A SINGLE SEPARABLE INTERACTION

The basic equation to be solved is the BCS integral equation[1] (for notation, see Ref. 6; however, we use here Δ_k for the quantity Δ_k^0)

$$\Delta_k=-\tfrac{1}{2}\sum_{k'}\frac{\Delta_{k'}G_{k,k'}^0}{(\hat{e}_{k'}^2+\Delta_{k'}^2)^{1/2}}.$$

The energy gap is interpreted as $2\Delta_{k_F}\equiv2\Delta$. $\hat{e}_{k'}$ is a renormalized single-particle energy measured with respect to the Fermi energy and $G_{k,k'}^0$ is the free-particle-interaction matrix element

$$G_{k,k'}^0=\langle\mathbf{k},-\mathbf{k}|V|\mathbf{k}',-\mathbf{k}'\rangle.$$

Throughout this paper only the s-wave part of this matrix is used, and $\hat{e}_k$ is represented by the effective-

* Supported in part by the U. S. Atomic Energy Commission under Contract A.T.(45-1)1388, Program B.

[1] J. Bardeen, L. N. Cooper, and J. R. Schrieffer, Phys. Rev. **108**, 1175 (1957).

[2] A. Bohr, B. R. Mottelson, and D. Pines, Phys. Rev. **110**, 936 (1958).

[3] L. N. Cooper, R. L. Mills, and A. M. Sessler, Phys. Rev. **114**, 1377 (1959).

[4] R. L. Mills, A. M. Sessler, S. A. Moszkowski, and D. G. Shankland, Phys. Rev. Letters **3**, 381 (1959).

[5] V. J. Emery and A. M. Sessler, Phys. Rev. **119**, 248 (1960).

[6] E. M. Henley and L. Wilets, preceding paper, Phys. Rev. **133**, B1118 (1964).